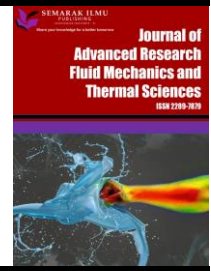




Journal of Advanced Research in Fluid Mechanics and Thermal Sciences

Journal homepage:
https://semarakilmu.com.my/journals/index.php/fluid_mechanics_thermal_sciences/index
ISSN: 2289-7879



Investigating the Effect of Deacetylation Temperature on the Characterization of Chitosan from Crab Shells as a Candidate for Organic Nanofluids

Rifky Ismail^{1,2,*}, Deni Fajar Fitriyana^{3,*}, Athanasius Priharyoto Bayuseno¹, Jamari¹, Putut Yoga Pradiptya^{1,2}, Rilo Chandra Muhamadin^{1,2}, Fariz Wisda Nugraha^{1,2}, Rusiyanto³, Andri Setiyawan³, Aldias Bahatmaka³, Hendrix Noviyanto Firmansyah³, Samsudin Anis³, Agustinus Purna Irawan⁴, Januar Parlaungan Siregar⁵, Tezara Cionita⁶

¹ Mechanical Engineering Dept. Diponegoro University, Semarang, Indonesia

² Center for Biomechanics, Biomaterial, Biomechatronics, and Biosignal Processing, Diponegoro University, Semarang, Indonesia

³ Mechanical Engineering Dept. Universitas Negeri Semarang, Semarang, Indonesia

⁴ Faculty of Engineering, Universitas Tarumanagara, Jakarta Barat 11440, Indonesia

⁵ Colleges of Engineering, Universiti Malaysia Pahang, 26300 Gambang, Kuantan, Malaysia

⁶ Department of Mechanical Engineering, Faculty of Engineering and Quantity Surveying, INTI International University, 71800 Nilai, Negeri Sembilan, Malaysia

ARTICLE INFO

Article history:

Received 7 October 2022

Received in revised form 26 January 2023

Accepted 3 February 2023

Available online 20 February 2023

Keywords:

Demineralization; deproteination; deacetylation; chitosan; crab shell waste; scaffold

ABSTRACT

Chitosan has been broadly utilized in bone scaffold production because of its antibacterial qualities, low toxicity, biodegradability, biocompatibility, and ability to aid regeneration processes in wound healing. In this work, chitosan was produced from crab shell waste through demineralization, deproteination, and deacetylation, utilizing HCl 1:7 (v/v), NaOH 3%, 1:10 (v/w), and NaOH 50%. The aim of this study is to examine the deacetylation temperature's impact towards the crystallinity index, chemical bond, degree of deacetylation, and morphology of chitosan synthesized. The deacetylation procedure was conducted for eight hours at temperatures of 100°C, 120°C, and 140°C. The synthesized chitosan was evaluated by utilizing XRD, FTIR, and SEM methods. According to the findings of this investigation, deacetylation at a temperature of 140 °C produced the highest degree of deacetylation, resulting in the highest quality chitosan. In addition, compared to other obtained chitosans, the shape of this result of synthesis is homogenous. At a deacetylation temperature of 140°C, the amounts of deacetylation degree, and crystallinity index of the chitosan were, in order, 81%, and 44%.

* Corresponding author.

E-mail addresses: r.ismail.undip@gmail.com

* Corresponding author.

E-mail addresses: deniifa89@mail.unnes.ac.id

<https://doi.org/10.37934/arfmts.103.2.5567>

1. Introduction

Crabs are marine invertebrates (crustaceans) that have high economic value and are an important commodity for Indonesia, especially in the fisheries sector. It is a fishery commodity with a reasonably high selling value.

Since the 1990s, crabs have become one of the export commodities that increase yearly [1]. The crab industry usually only takes the meat and discards the shell. The by-product of processing crab meat is 57% shell waste (skin and head) [2]. In Indonesia, this shell waste has not been utilized optimally, resulting in unpleasant odors and water pollution that impact the environment. The utilization of waste marine products, such as crab shell proffers environmental and financial advantages gained from waste recovery. This is because it is cheap, available in large quantities, and can be easily obtained [3-7]. The three main components of the crab shell are 15% - 20% chitin, 25% - 44% protein, 45% - 50% calcium carbonate [8]. Chitin also knowns as the homopolymer of Beta-(1,4)-N-acetyl-D-glucosamine. Its structure is very similar to cellulose, except that a hydroxyl group replaces the acetamido group on the second carbon atom. Chitin polymers are microfibrils about 3 nm in diameter stabilized by hydrogen bonds between amine and carboxyl groups [9].

Several studies have shown that crab shells contain chitin which can be converted into chitosan through deacetylation reactions. Chitosan is produced from chitin with the same chemical structure consisting of a protracted molecular chain and a hovering molecular weight [10-12]. A difference between chitin and chitosan is that in every chitin molecule's ring, there lays an acetyl group (-CH₃-CO) on the secondary carbon atom, whereas, in chitosan, there is an amine group (-NH) [13]. Chitosan is solely a basic polysaccharide amongst nature, whereas the remains, such as agar, alginic acid, carrageenan, cellulose, dextran, pectin, and starch, are acidic or neutral.

Chitosan has non-toxic, odorless, biodegradable, and biocompatible characteristics. Chitosan acts as a biocompatible substance that degrades gradually into wholesome goods (amino sugars) completely engrossed in the body. Chitosan is being hydrolyzed by lysozyme to oligomers that activate macrophages to produce *N*-acetyl-*D*-glucosamide, which catalyzes the production of NAG, *D*-glucosamine, and substituted glucosamine from oligomers. The hydrolyzation happens in vivo [14]. The physical and chemical properties of chitosan rely on the molecular weight (MW), deacetylation degree (DD), degree of crystallinity, degree of ionization, free amino groups, and others. Chitosan has three different types of reactive functional groups at the locations of C-2, C-3, and C-6: amino or acetamido groups, primary and secondary hydroxyl groups, and others. Due to their intra- and intermolecular hydrogen bonds, amino groups are in charge of physicochemical qualities and structural variations.

Chitosan has been widely used as a non-parental drug delivery system in wound dressings because it is biodegradable and biocompatible [15]. With its cellulose-like structure, chitosan is a biopolymer that can increase wound healing ratio, support cell growth, and is effective for tissue engineering. Chitosan also exhibits bacteriostatic and fungistatic properties that prevent infection. The food industry uses chitooligosaccharides and chitosan (edible varieties with more than 83% DD) as dietary food supplements. Due to its capacity to bind fat, it also serves as a dietary supplement to prevent obesity. [16]. The chitosan fiber that is binding the fat creates a mass that the human body cannot either absorb or expel. Chitosan fiber forms a negative-charged chemical bond with fats, lipids, and bile acids. It has also been reported that chitosan lowers cholesterol (hypocholesterolemic) [17,18]. In addition to its applications in the medical field, chitosan can also be used as a surfactant and can reduce fluid viscosity so as to provide higher thermal conductivity. Modi *et al.*, [15] used chitosan as an organic nanofluid in solar water heating systems because it has better thermal properties than aluminum oxide, which is used as an inorganic nanofluid. The results

of their research showed that chitosan had the highest heat removal factor, at 0.627. Chitosan, aluminum oxide, and water had experimental efficiencies of 55.86%, 52.72%, and 41.81%, respectively. This study aims to synthesize chitosan from crab shell waste by deproteinization, demineralization, and deacetylation. It also aims at determining the effect of deacetylation temperature on the physical and morphological properties of the resulting chitosan.

2. Materials and Methods

This study shows a chitosan that was synthesized from the crab shell waste (Figure 1) through demineralization, deproteinization, and deacetylation.

Figure 2 shows the experimental setup used in this research. The shells were obtained from the crab consumption waste in Semarang, Central Java. Chitosan synthesis was started by size reduction of the crab shells using a blender. The shells were crushed into powder, and then filtered using mesh 100. This process involved XRD, FTIR, and EDX tests to determine the shell powder's crystalline phase, chemical bonding, and chemical composition.



Fig. 1. Crab shells for synthesis chitosan

To remove the protein found in the crab shells, 100 grams of crab shell powder are deproteinized with 3% NaOH 1:10 (v/w) and swirled with a magnetic stirrer at 90°C for an hour. After being washed to a neutral pH, the powder is dried in an oven. The result of deproteinization from 100 g of crab shell powder is 89.94 g. The synthesis process is continued with demineralization to separate minerals or inorganic compounds from the crab shell powder. The process uses HCl 1:7 (w/v) with a magnetic stirrer at 90°C for 1 hour. After washing until the pH is neutral, the powder is dried using the oven. The result of demineralization from 89.94 grams of crab powder is 79.27 grams. The last process of chitosan synthesis is deacetylation using 50% NaOH with 1:20 (w/v) ratio for 8 hours at 100°C, 120°C, and 140°C. 20 grams of powder resulting from the demineralization process is utilized in the deacetylation process. Breaking the connection between the nitrogen atom and the acetyl group to convert it to an amine group is the goal of the deacetylation process (-NH₂). After this process, the residue (solid particles) is cooled, filtered, washed, and dried.

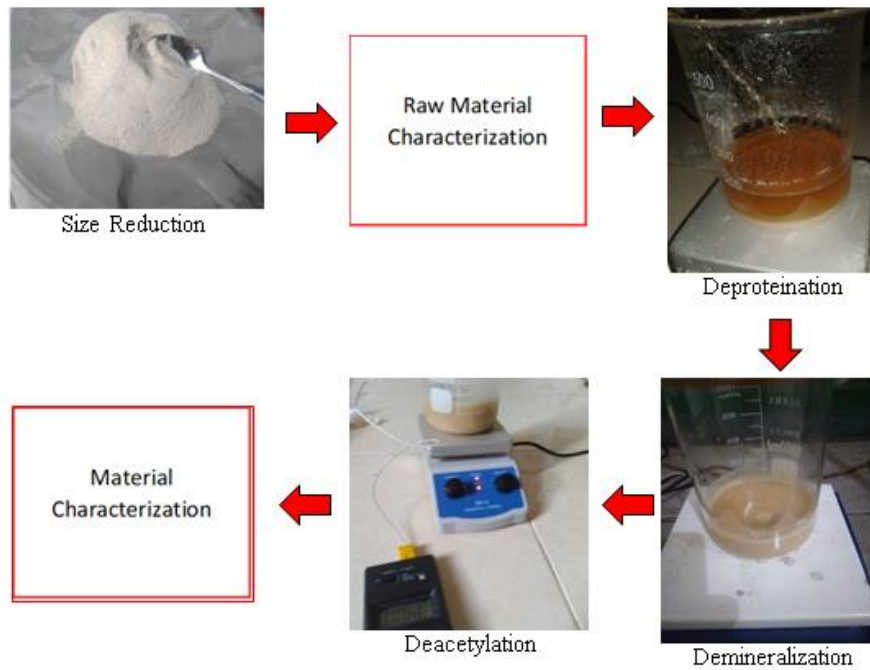


Fig. 2. The experimental setup

After the synthesis process is complete, it is continued with the characterization of chitosan to observe the chitosan properties through XRD, SEM, and FTIR tests. The resulting chitosan's crystal phase and crystallinity index were determined using XRD analysis [19,20]. XRD samples were prepared on the plate in the concave to the brim part and then flattened using a glass before being inserted into the XRD. The surface characteristics of chitosan from crab shells were observed using SEM with 30000x magnification.

FTIR is a method for measuring the infrared spectrum of solid, liquid, and gas sample absorption, emission, and photoconductivity [19,20]. It is also able to detect various functional groups in chitosan. The deacetylation degree (DD) was analyzed using a histogram from the FTIR test [21]. The deacetylation degree measurement is based on the spectrophotometer's curve. The highest peak (P0) and lowest peak (P) were recorded and measured with the selected baseline. The following formula is used to calculate the absorbance ratio [22,23]

$$A = \log\left(\frac{P_0}{P}\right) \quad (1)$$

where,

A = Absorbance ratio

P0 = The distance between the baseline and the tangent that connects the two highest peaks with a wavelength of 1655cm^{-1}

P = The the distance between the baseline and the lowest valley with a wavelength of 1655cm^{-1} or 3450cm^{-1} .

By measuring the absorbance at the corresponding peak, the percent value of Deacetylation Degree (DD) can be calculated using the following formula [22,23]

$$DD = \left[1 - \left(\frac{A_{1655}}{A_{3450}} \times \frac{1}{1.33}\right)\right] \times 100\% \quad (2)$$

where,

DD = deacetylation degree (%)

A_{1655} = Absorbance at the wavelength of 1655 cm^{-1}

A_{3450} = Absorbance at the wavelength of 3450 cm^{-1}

1.33 = Constant for the perfect deacetylation degree.

3. Results and Discussion

3.1 Crab Shells Characterization

Figure 3 shows the FTIR test results for crab shell powder. CaCO_3 compounds can be characterized based on the peaks at wave numbers $1400 - 1500\text{ cm}^{-1}$. This figure indicates the presence of C–O bonds, which is a typical signal for carbonate compounds [24]. In this study, the bands $864.1 - 711.14\text{ cm}^{-1}$ and $1473.62 - 1392.22\text{ cm}^{-1}$ in the FTIR spectrum of calcium carbonate correlate to the Ca–O and C–O bonds. This is consistent with the high CaCO_3 concentration in the crab shells sample. Based on the characteristics of the resulting peak, FTIR results can also identify the type of crystal that has formed. Aragonite is responsible for the large absorption bands between 700 and 900 cm^{-1} . Calcite is characterized by absorption bands at approximately 1416.862 and 706 cm^{-1} [24,25].

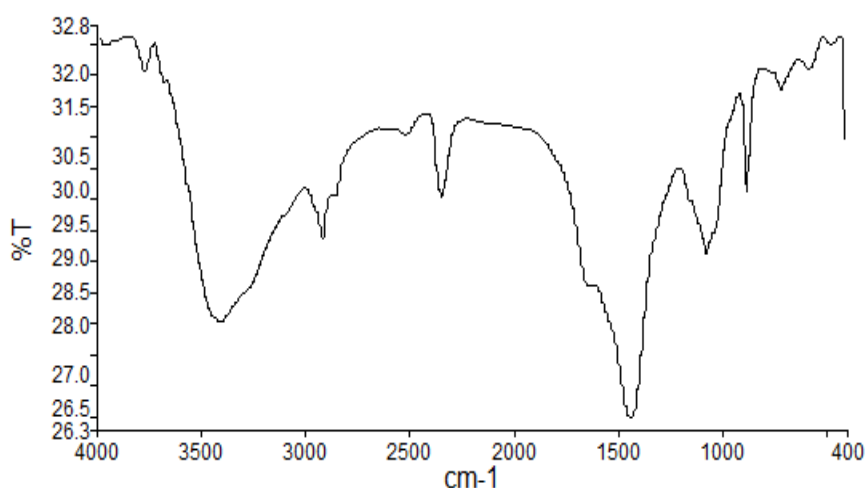


Fig. 3. FTIR spectra of crab shell powder

The FTIR test results are consistent with the XRD test results. XRD data were analyzed qualitatively for the purpose of examining crab shell powder samples. As a result, the standard powder diffraction database from the International Centre for Diffraction Data was used to match intensity lines seen in XRD spectra with the mineral database (ICDD). Figure 4 displays XRD patterns of crystalline phases in crab shell powder samples. The calcium carbonate peak spectra in the powdered crab mussel shells have intensities at 2θ of 26.233° , 27.238° , and 45.881° , and they connect with aragonite peak intensities that match ICDD#PDF760606 [24].

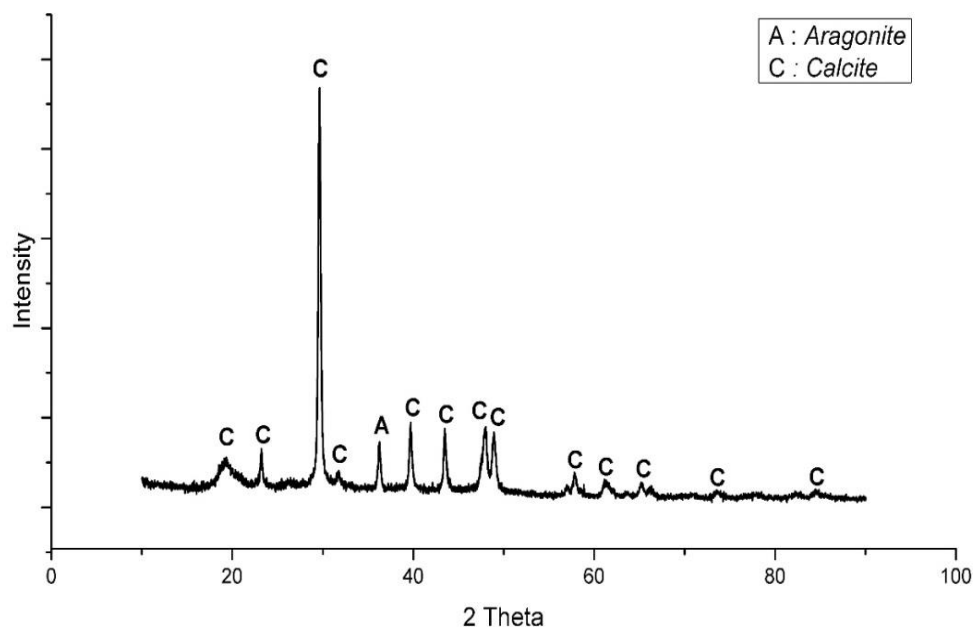


Fig. 4. X-ray diffractograms of Crab Shell powder

EDS, EDAX, or Energy Dispersive X-Ray Analysis (EDX) are further names for the x-ray technique that may identify the elements that make up a material. From the results of the EDX test, there are impurities of Na, Mg, P, and Zr of 0.38%, 1.40%, 3.33%, and 1.99%, respectively. Impurities such as Na, Mg, P, and Zr probably came from the content of the shell itself. Table 1 lists the elements that make up the crab shell powder. From the results of the EDX test, there are impurities of Na, Mg, P, and Zr of 0.38%, 1.40%, 3.33%, and 1.99%, respectively. Impurities such as Na, Mg, P, and Zr probably came from the content of the shell itself.

Table 1
 Elemental composition of crab shell powder

Element	Mass (%)
C	29.44
O	38.97
Na	0.38
Ca	24.49
Mg	1.40
P	3.33
Zr	1.99
Total	100.00

3.2 Chitosan Characterization

There is shown the material characterization data by the X-Ray Diffraction method with intensity and angle 2θ (Figure 4). Meanwhile, the X-Ray Diffraction data are read and analyzed by matching the data with X-ray diffraction patterns in JCPDS-ICDD and literature. Chitosan peak data was compared with JCPDS data number 39-1894, which stated that the highest peaks of chitosan were shown at 2θ of 15.18, 20.3, 21.2, 23.9, and 29.9.

Using the origin program, the crystallinity index is determined as the ratio of the total area under the XRD peaks to the area of the crystal contribution [26]. The following formula is used to calculate the crystallinity index [26,27]

$$\text{Crystallinity Index (\%)} = \frac{\text{area of crystalline peak}}{\text{area of all peak}} \times 100\% \quad (3)$$

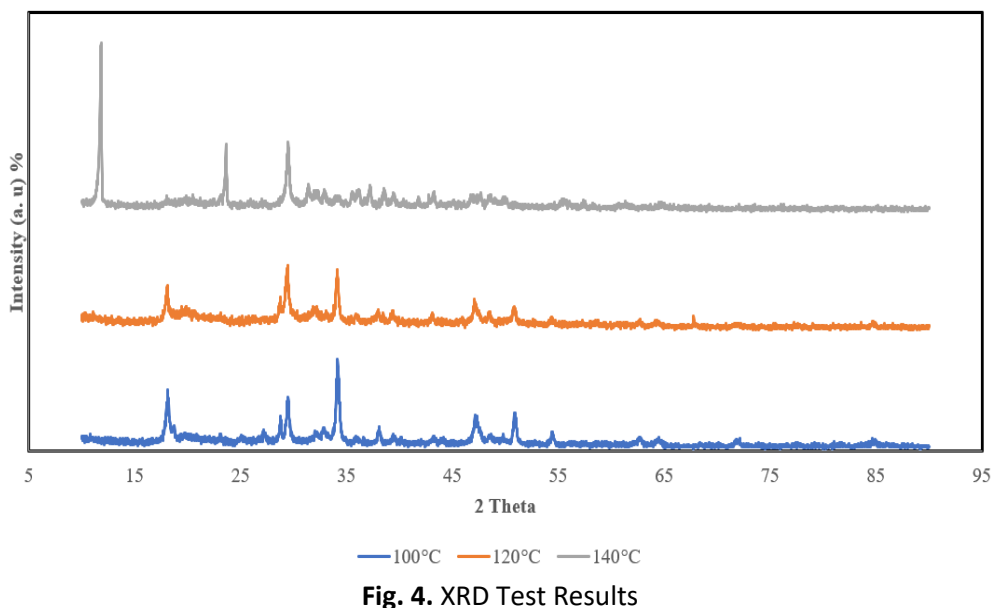


Fig. 4. XRD Test Results

The high deacetylation temperature decreases the chitosan crystallinity index (Figure 5). Deacetylation induces heterogeneity in the molecular chain, hence decreasing crystallinity [28]. The peak enlargement on XRD graphs is influenced by heterogeneous polymer chain structure, macromolecular regularity level, and crystallinity levels [29]. This research produced chitosan in which the amorphous phase predominated over the crystalline phase. The amorphous structure can lower the melting point of pharmaceutical substances, hence requiring less energy to dissolve them than the crystal structure with a regular lattice [30]. The simplest explanation for the aforementioned difference in the degree of crystallinity is different distribution patterns of residual acetamide groups in macromolecules of the two examined polysaccharides [31]. On the grounds that the random distribution of acetamido and amino groups, amorphous chitosan has weaker intermolecular interactions and is, therefore, easier to dissolve [32,33].

Figure 6 shows a graphical comparison of the FTIR test results of chitosan synthesis with temperature variations in the deacetylation process. The FTIR characterization results were compared with the wavelengths from the research by Pambudi *et al.*, [34] and Rumengan *et al.*, [35] as a reference in determining the functional groups of the resulting chitosan. The FTIR spectra of chitosan exhibit many peaks, according to Pambudi. Wave numbers 2920, 2891, 2992, 2882, and 2924 cm^{-1} imply aliphatic (CH)(-CH₂) vibration, while wave numbers 3449, 3447, 3445, 3462, and 3430 cm^{-1} denote vibrations of the hydroxyl (-OH) group. Wave numbers 1381, 1383, 1400, 1414 cm^{-1} represent methyl group (-CH₃) vibration, wave numbers 1076, 1082, 1080, 1076, and 1059 cm^{-1} indicate vibrations of (-COC-) group, and wave numbers 1643, 1635, 1641, 1640, and 1651 cm^{-1} reveal a bending vibration of the amide group (NH₂). The comparison of the peaks of the FTIR test findings is shown in Table 2.

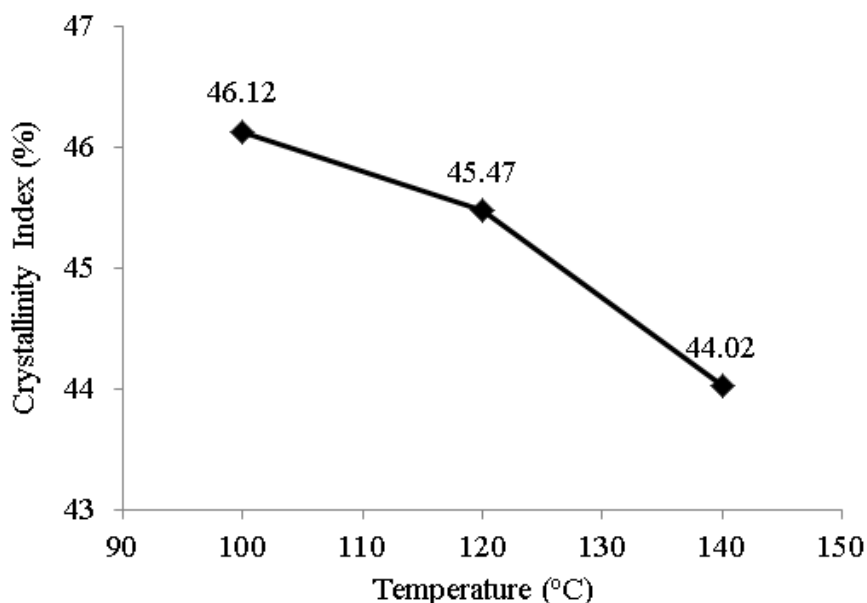


Fig. 5. The influence of the deacetylation temperature on the crystallinity index of obtained chitosans

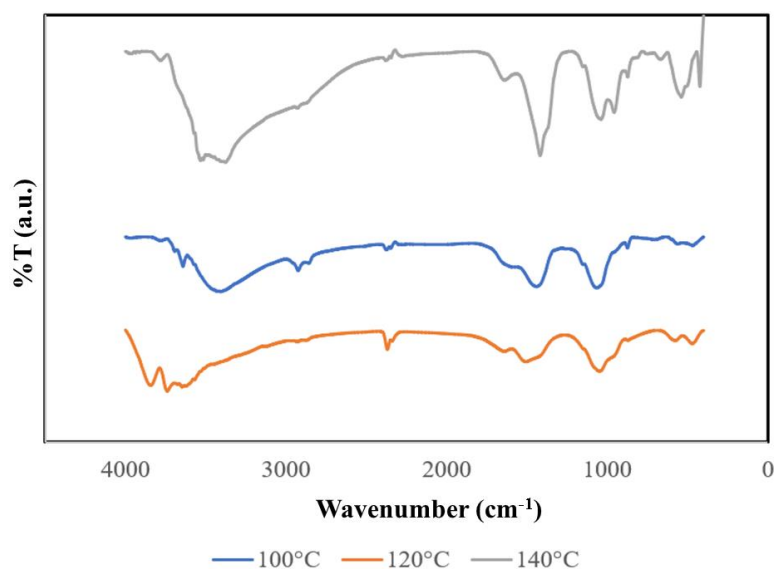


Fig. 6. FTIR test results on obtained chitosan

There are absorption peaks in the range of 3432 cm^{-1} (chitosan O-H stretching vibration), 2924 cm^{-1} (chitosan C-H bending vibration), 1650 cm^{-1} (bending vibration of NH_2 cutting), 1439 cm^{-1} (CH_3 stretching vibration), and 1069 cm^{-1} in the FTIR spectra of chitosan at 100°C (C-O-C stretching vibration). Chitosan exhibits absorption peaks in the region of 3455 cm^{-1} (O-H stretching vibration of chitosan), 2882 cm^{-1} (C-H stretching vibration), 1648 cm^{-1} (NH_2 bending vibration), 1277 cm^{-1} (CH_3 bending vibration), and 1051 cm^{-1} in the FTIR spectrum at 120°C (C-O-C stretching vibration). Additionally, there are absorption peaks in the range of 3451 cm^{-1} (chitosan O-H stretching vibration), 2891 cm^{-1} (chitosan C-H stretching vibration), 1642 cm^{-1} (NH_2 bending vibration), 1419 cm^{-1} (CH_3 bending vibration), and 1151 cm^{-1} in the FTIR spectra of chitosan at 140°C (C-O-C stretching vibration).

Table 2
The comparison of FTIR test results

Functional Group	Deacetylation Product		
	100°C	120°C	140°C
-OH	3432	3455	3451
-CH stretching	2924	2882	2891
-NH2 cutting	1650	1648	1642
-CH3	1439	1277	1419
-C-O-C-	1069	1051	1151

The deacetylation temperature influences the degree of deacetylation of the obtained chitosan. As seen in Figure 7, the degree of deacetylation raises as the deacetylation temperature rises. The deacetylation reaction rate is proportional to the deacetylation temperature because intermolecular mobility is increased by increasing the deacetylation temperature, hence accelerating the acetyl group termination reaction [36]. Chitosan produced at deacetylated temperatures of 100 and 120°C is categorized as the low deacetylated degree of chitosan because it has a DD in the range of 55-77%. Meanwhile, chitosan produced at a deacetylated temperature of 140°C is categorized as a middle deacetylated degree of chitosan because it has a DD in the range of 70-85%. At a low deacetylated degree of chitosan, it is almost completely insoluble in water. However, at the middle deacetylated degree of chitosan may be partially dissolved in water [36,37].

The quantity of acetyl groups removed from the polysaccharide, leaving free amino groups, is indicated by the deacetylation degree (DD) of chitosan. The more accessible amine groups there are, the more potential there is for them to act as binding sites for contaminants. The DD of synthesized chitosan is significantly influenced by temperature, the length of the reaction, and the amount of NaOH. In 6 hours, Kumari *et al.*, [38] synthesized chitosan from fish scales, shrimp shells, and crab shells using 40% KOH at various temperatures. At the 80, 100, and 120 °C, the DD was reported to be 73.05, 95.97, and 90.17 %. Mathaba *et al.*, [39] synthesized chitosan with reaction duration was held constant at 6 hours, while temperature (80 °C, 100 °C, and 120 °C) and NaOH concentration (20 percent, 40 percent, and 60 percent) were altered to synthesize chitosan samples with varying DD. In the current investigation, when the temperature was increased from 100°C to 140°C, the DD increased from 62% to 82% while the NaOH concentration stayed constant at 50%. The following is a result of the increased kinetic energy caused by higher temperatures, which degrades acetyl groups as more reactions occur. More amine groups are exposed when more acetyl groups are removed, increasing the DD of the chitosan [38-40]. The deacetylation degree also correlated with the particle size of chitosan. A higher % DD produces chitosan with larger particle size [41].

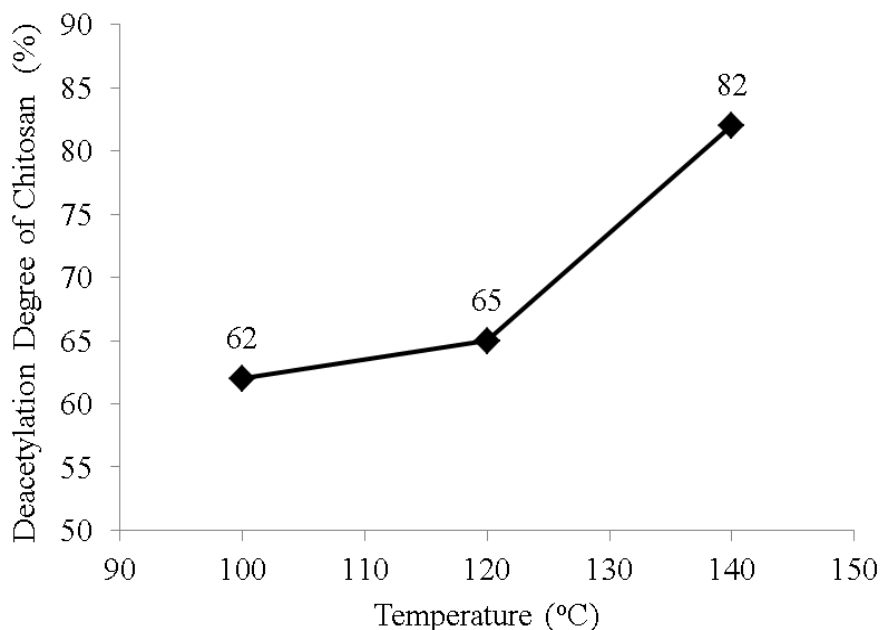


Fig. 7. The influence of the deacetylation temperature on the crystallinity index of obtained chitosans

Characterization by Scanning Electron Microscope (SEM) is required in this study to determine the synthesized chitosan's morphology. Figure 8 presents the morphology of the SEM results of deacetylated chitosan. A variety of large and small, spherical, cube-like objects with a hazy appearance were visible in the crab chitosan SEM images. Chitosan formed a rough, needle-like structure after being deacetylated at a temperature of 140°C, where uneven granules vanished.

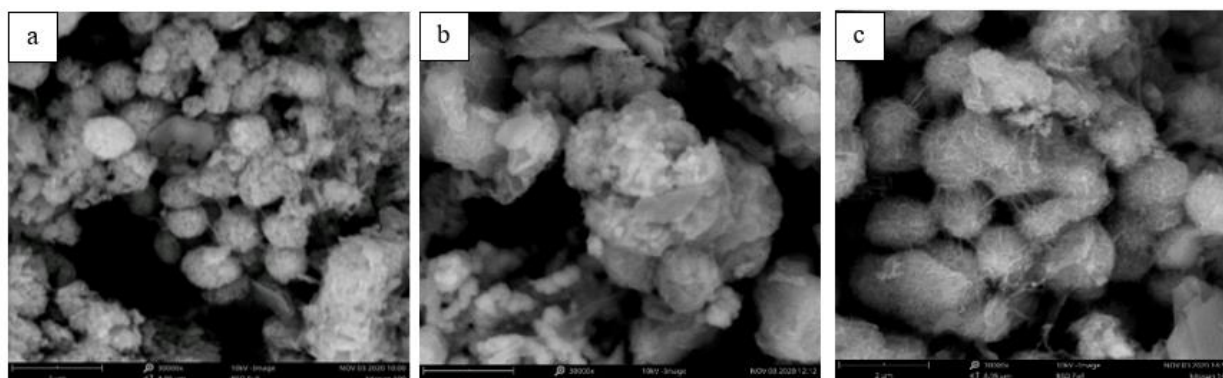


Fig. 8. SEM Results with 30000x magnification of surface morphology of deacetylated chitosan at 100°C (a), 120°C (b), 140°C (c)

4. Conclusion

Chitosan as a whole was successfully synthesized using crab shells. The best chitosan was produced by deacetylation at 140°C for 8 hours with a deacetylation degree of 82%. The temperature of the deacetylation influences the synthesis of chitosan. A higher deacetylation temperature will produce a lower crystallinity index and a higher deacetylation degree. Temperature affects the deacetylation degree because with a higher deacetylation temperature, the reaction rate gets higher either. Temperature can increase the intermolecular motion, so the acetyl group termination reaction will run faster.

Acknowledgement

The authors express the gratitude for the research funding from Hibah Strategis 2023, Faculty of Engineering, Diponegoro University. The initial research and material preparation was funded by the CBIOM3S Diponegoro University from the research grant for center of excellence, Ministry of Education, Culture, Research and Technology RI.

References

- [1] Kembaren, Duranta Diandria, Tri Ernawati, and Suprpto Suprpto. "Biologi dan parameter populasi rajungan (*portunus pelagicus*) di perairan bone dan sekitarnya." *Jurnal penelitian perikanan Indonesia* 18, no. 4 (2016): 273-281.
- [2] Hastuti, Sri, Syamsul Arifin, and Darimiyya Hidayati. "Pemanfaatan limbah cangkang rajungan (*Portunus pelagicus*) sebagai Perisa Makanan Alami." *Agrointek: Jurnal Teknologi Industri Pertanian* 6, no. 2 (2012): 88-96.
- [3] Prihanto, A., S. Muryanto, R. Ismail, J. Jamari, and A. P. Bayuseno. "Practical insights into the recycling of green mussel shells (*Perna Viridis*) for the production of precipitated calcium carbonate." *Environmental Technology* (2022): 1-11. <https://doi.org/10.1080/09593330.2022.2103458>
- [4] Fitriyana, Deni Fajar, Rifky Ismail, Yanuar Iman Santosa, Sri Nugroho, Ahmad Jazilussurur Hakim, and Mohammad Syahreza Al Mulqi. "Hydroxyapatite synthesis from clam shell using hydrothermal method: A review." In *2019 International Biomedical Instrumentation and Technology Conference (IBITeC)*, vol. 1, pp. 7-11. IEEE, 2019. <https://doi.org/10.1109/IBITeC46597.2019.9091722>
- [5] Ismail, Rifky, Muhammad Bagus Laroybafih, Deni Fajar Fitriyana, Sri Nugroho, Yanuar Iman Santoso, Ahmad Jazilussurur Hakim, Mohammad Syahreza Al Mulqi, and Athanasius Priharyoto Bayuseno. "The effect of hydrothermal holding time on the characterization of hydroxyapatite synthesized from green mussel shells." *Journal of Advanced Research in Fluid Mechanics and Thermal Sciences* 80, no. 1 (2021): 84-93. <https://doi.org/10.37934/arfmts.80.1.8493>
- [6] Fitriyana, D. F., F. W. Nugraha, M. B. Laroybafih, R. Ismail, A. P. Bayuseno, R. C. Muhamadin, M. B. Ramadan, A. RA Qudus, and J. P. Siregar. "The effect of hydroxyapatite concentration on the mechanical properties and degradation rate of biocomposite for biomedical applications." In *IOP Conference Series: Earth and Environmental Science*, vol. 969, no. 1, p. 012045. IOP Publishing, 2022. <https://doi.org/10.1088/1755-1315/969/1/012045>
- [7] Ismail, Rifky, D. F. Fitriyana, Y. I. Santosa, S. Nugroho, A. J. Hakim, M. S. Al Mulqi, J. Jamari, and A. P. Bayuseno. "The potential use of green mussel (*Perna Viridis*) shells for synthetic calcium carbonate polymorphs in biomaterials." *Journal of Crystal Growth* 572 (2021): 126282. <https://doi.org/10.1016/j.jcrysgro.2021.126282>
- [8] Sukma, Sari, Sri Eva Lusiana, Masruri Masruri, and Suratmo Suratmo. "Kitosan dari rajungan lokal *Portunus pelagicus* asal Probolinggo, Indonesia." PhD diss., Brawijaya University, 2014.
- [9] Gooday, G. W. "The ecology of chitin degradation. Di dalam: Marshall KC, editor *Advances in Microbial Ecology*." (1994): 378-430.
- [10] Abd Razak, Noor Harliza, Nur Wahida Mohd Shukori, and Ku Halim Ku Hamid. "Elemental Analysis of Chitin from Extraction of Different Ages of *Leucaena Leucephala* with Hydrochloric Acid." *Journal of Advanced Research in Applied Sciences and Engineering Technology* 16, no. 1 (2019): 20-25.
- [11] Abd Razak, Noor Harliza, Siti Nadzirah Mohd Nawi, and Ku Halim Ku Hamid. "Characterization Of Chitin With Extraction *Leucaena Leucephala* Pods Using Hydrochloric Acid (HCl) By Fourier Transform Infrared." *Journal of Advanced Research in Applied Sciences and Engineering Technology* 17, no. 1 (2019): 21-28.
- [12] Majnis, Mohd Fadhil, Mei Mei Chong, Ku Zilati Ku Shaari, and Mohd Azam Mohd Adnan. "Wettability Study of Chitosan Droplet on Surface-Modified PDMS for Microfluidics Application." *Progress in Energy and Environment* 12 (2020): 22-29.
- [13] Supriyantini, Endang, Bambang Yulianto, Ali Ridlo, Sri Sedjati, and Amtoni Caesario Nainggolan. "Pemanfaatan chitosan dari limbah cangkang rajungan (*Portunus pelagicus*) sebagai adsorben logam timbal (Pb)." *Jurnal Kelautan Tropis* 21, no. 1 (2018): 23-28. <https://doi.org/10.14710/jkt.v21i1.2399>
- [14] Singh, Dinesh K., and Alok R. Ray. "Biomedical applications of chitin, chitosan, and their derivatives." *Journal of Macromolecular Science, Part C: Polymer Reviews* 40, no. 1 (2000): 69-83. <https://doi.org/10.1081/MC-100100579>
- [15] Modi, Kalpesh, Dhruvin Shukla, Brijesh Bhargav, Jayesh Devaganiya, Rahul Deshle, Jaysukh Dhodi, Dhruvil Patel, and Alpesh Patel. "Efficacy of organic and inorganic nanofluid on thermal performance of solar water heating system." *Cleaner Engineering and Technology* 1 (2020): 100020. <https://doi.org/10.1016/j.clet.2020.100020>
- [16] Ramya, R., Jayachandran Venkatesan, Se Kwon Kim, and P. N. Sudha. "Biomedical applications of chitosan: an overview." *Journal of Biomaterials and Tissue Engineering* 2, no. 2 (2012): 100-111.

- <https://doi.org/10.1166/jbt.2012.1030>
- [17] Xia, Wenshui, Ping Liu, Jiali Zhang, and Jie Chen. "Biological activities of chitosan and chitoooligosaccharides." *Food hydrocolloids* 25, no. 2 (2011): 170-179. <https://doi.org/10.1016/j.foodhyd.2010.03.003>
- [18] van der Gronde, Toon, Anita Hartog, Charlotte van Hees, Hubert Pellikaan, and Toine Pieters. "Systematic review of the mechanisms and evidence behind the hypocholesterolaemic effects of HPMC, pectin and chitosan in animal trials." *Food chemistry* 199 (2016): 746-759. <https://doi.org/10.1016/j.foodchem.2015.12.050>
- [19] Ismail, Rifky, Muhammad Bagus Laroybafih, Deni Fajar Fitriyana, Sri Nugroho, Yanuar Iman Santoso, Ahmad Jazilussurur Hakim, Mohammad Syahreza Al Mulqi, and Athanasius Priharyoto Bayuseno. "The effect of hydrothermal holding time on the characterization of hydroxyapatite synthesized from green mussel shells." *Journal of Advanced Research in Fluid Mechanics and Thermal Sciences* 80, no. 1 (2021): 84-93. <https://doi.org/10.37934/arfmts.80.1.8493>
- [20] Fitriyana, D. F., Hazwani Suhaimi, R. Noferi, and Wahyu Caesarendra. "Synthesis of Na-P Zeolite from geothermal sludge." In *NAC 2019: Proceedings of the 2nd International Conference on Nanomaterials and Advanced Composites*, pp. 51-59. Springer Singapore, 2020. https://doi.org/10.1007/978-981-15-2294-9_5
- [21] Domszy, Julian G., and George AF Roberts. "Evaluation of infrared spectroscopic techniques for analysing chitosan." *Die Makromolekulare Chemie: Macromolecular Chemistry and Physics* 186, no. 8 (1985): 1671-1677. <https://doi.org/10.1002/macp.1985.021860815>
- [22] Zam, Z. Z., F. Muin, and A. Fataruba. "Identification of chitosan beads from coconut crab patani variety using Fourier transform infrared spectroscopy (FTIR)." In *Journal of Physics: Conference Series*, vol. 1832, no. 1, p. 012014. IOP Publishing, 2021. <https://doi.org/10.1088/1742-6596/1832/1/012014>
- [23] Ibitoye, E. B., I. H. Lokman, M. N. M. Hezmee, Y. M. Goh, A. B. Z. Zuki, and A. A. Jimoh. "Extraction and physicochemical characterization of chitin and chitosan isolated from house cricket." *Biomedical Materials* 13, no. 2 (2018): 025009. <https://doi.org/10.1088/1748-605X/aa9dde>
- [24] Ismail, Rifky, D. F. Fitriyana, Y. I. Santosa, S. Nugroho, A. J. Hakim, M. S. Al Mulqi, J. Jamari, and A. P. Bayuseno. "The potential use of green mussel (*Perna Viridis*) shells for synthetic calcium carbonate polymorphs in biomaterials." *Journal of Crystal Growth* 572 (2021): 126282. <https://doi.org/10.1016/j.jcrysgro.2021.126282>
- [25] Vagenas, N. V., A. Gatsouli, and C. G. Kontoyannis. "Quantitative analysis of synthetic calcium carbonate polymorphs using FT-IR spectroscopy." *Talanta* 59, no. 4 (2003): 831-836. [https://doi.org/10.1016/S0039-9140\(02\)00638-0](https://doi.org/10.1016/S0039-9140(02)00638-0)
- [26] Park, Sunkyu, John O. Baker, Michael E. Himmel, Philip A. Parilla, and David K. Johnson. "Cellulose crystallinity index: measurement techniques and their impact on interpreting cellulase performance." *Biotechnology for biofuels* 3 (2010): 1-10. <https://doi.org/10.1186/1754-6834-3-10>
- [27] Dome, Karina, Ekaterina Podgorbunskikh, Aleksey Bychkov, and Oleg Lomovsky. "Changes in the crystallinity degree of starch having different types of crystal structure after mechanical pretreatment." *Polymers* 12, no. 3 (2020): 641. <https://doi.org/10.3390/polym12030641>
- [28] Cheng, Jiaqi, Huaping Zhu, Jianlian Huang, Jianxin Zhao, Bowen Yan, Shenyan Ma, Hao Zhang, and Daming Fan. "The physicochemical properties of chitosan prepared by microwave heating." *Food Science & Nutrition* 8, no. 4 (2020): 1987-1994. <https://doi.org/10.1002/fsn3.1486>
- [29] Ahmad, L. O., D. Permana, S. H. Wahab, L. O. Sabarwati, A. N. Ramadhan, and U. Rianse. "Improved chitosan production from tiger shrimp shell waste (*Penaeus mondon*) by multistage deacetylation method and effect of bleaching." *Adv Environ Geol Sci Eng.* *Adv. Environ. Geol. Sci. Eng.* (2015): 373-378.
- [30] Sari, Retno, Dwi Setyawan, Dini Retnowati, and Ririn Pratiwi. "Development of andrographolide-chitosan solid dispersion system: Physical characterization, solubility, and dissolution testing." *Asian journal of pharmaceuticals* 13, no. 1 (2019): 5-9.
- [31] Mogilevskaya, E. L., T. A. Akopova, A. N. Zelenetskii, and A. N. Ozerin. "The crystal structure of chitin and chitosan." *Polymer Science Series A* 48 (2006): 116-123. <https://doi.org/10.1134/S0965545X06020039>
- [32] Feng, Fang, Yu Liu, Binyuan Zhao, and Keao Hu. "Characterization of half N-acetylated chitosan powders and films." *Procedia Engineering* 27 (2012): 718-732. <https://doi.org/10.1016/j.proeng.2011.12.511>
- [33] Abdan, Khalina Binti, Soon Chu Yong, Eric Chan Wei Chiang, Rosnita A. Talib, Tan Choon Hui, and Lee Ching Hao. "Barrier properties, antimicrobial and antifungal activities of chitin and chitosan-based IPNs, gels, blends, composites, and nanocomposites." In *Handbook of Chitin and Chitosan*, pp. 175-227. Elsevier, 2020. <https://doi.org/10.1016/B978-0-12-817968-0.00006-8>
- [34] Pambudi, Galang B. Raka, Ita Ulfin, Harmami Harmami, Suprpto Suprpto, Fredy Kurniawan, and Yatim L. Ni'mah. "Synthesis of water-soluble chitosan from crab shells (*Scylla serrata*) waste." In *AIP Conference Proceedings*, vol. 2049, no. 1, p. 020086. AIP Publishing LLC, 2018. <https://doi.org/10.1063/1.5082491>
- [35] Rumengan, I. F. M., E. Suryanto, R. Modaso, S. Wullur, T. E. Tallei, and D. Limbong. "Structural characteristics of chitin and chitosan isolated from the biomass of cultivated rotifer, *Brachionus rotundiformis*." *Int. J. Fish. Aquat.*

- Sci 3, no. 1 (2014): 12-18.
- [36] Mastuti, Endang. "Pengaruh Konsentrasi NaOH dan Suhu pada Proses Deasetilasi Kitin dari Kulit Udang." *Ekuilibrum* 4, no. 1 (2005): 21-25. <https://doi.org/10.26874/jt.vol1no1.195>
- [37] Lv, S. H. "High-performance superplasticizer based on chitosan." In *Biopolymers and biotech admixtures for eco-efficient construction materials*, pp. 131-150. Woodhead Publishing, 2016. <https://doi.org/10.1016/B978-0-08-100214-8.00007-5>
- [38] Kumari, Suneeta, Sri Hari Kumar Annamareddy, Sahoo Abanti, and Pradip Kumar Rath. "Physicochemical properties and characterization of chitosan synthesized from fish scales, crab and shrimp shells." *International journal of biological macromolecules* 104 (2017): 1697-1705. <https://doi.org/10.1016/j.ijbiomac.2017.04.119>
- [39] Mathaba, Machodi, and Michael Olawale Daramola. "Effect of chitosan's degree of deacetylation on the performance of pes membrane infused with chitosan during amd treatment." *Membranes* 10, no. 3 (2020): 52. <https://doi.org/10.3390/membranes10030052>
- [40] Ahlafi, Hammou, Hamou Moussout, Fatima Boukhlifi, Mostafa Echetna, Mohamed Naciri Bennani, and Slimani My Slimane. "Kinetics of N-deacetylation of chitin extracted from shrimp shells collected from coastal area of Morocco." *Mediterranean Journal of Chemistry* 2, no. 3 (2013): 503-513. <https://doi.org/10.13171/mjc.2.3.2013.22.01.20>
- [41] Jampafuang, Yattra, Anan Tongta, and Yaowapha Waiprib. "Impact of crystalline structural differences between α - and β -chitosan on their nanoparticle formation via ionic gelation and superoxide radical scavenging activities." *Polymers* 11, no. 12 (2019): 2010. <https://doi.org/10.3390/polym11122010>



Scimago Journal & Country Rank

Enter Journal Title, ISSN or Publisher Name

- Home
- Journal Rankings
- Country Rankings
- Viz Tools
- Help
- About Us

Journal of Advanced Research in Fluid Mechanics and Thermal Sciences

COUNTRY

Malaysia



Universities and research institutions in Malaysia



Media Ranking in Malaysia

SUBJECT AREA AND CATEGORY

Chemical Engineering
Fluid Flow and Transfer Processes

PUBLISHER

Penerbit Akademia Baru

H-INDEX

17

PUBLICATION TYPE

Journals

ISSN


22897879


COVERAGE

2017-2021

SCOPE

Information not localized

 Join the conversation about this journal

 Quartiles

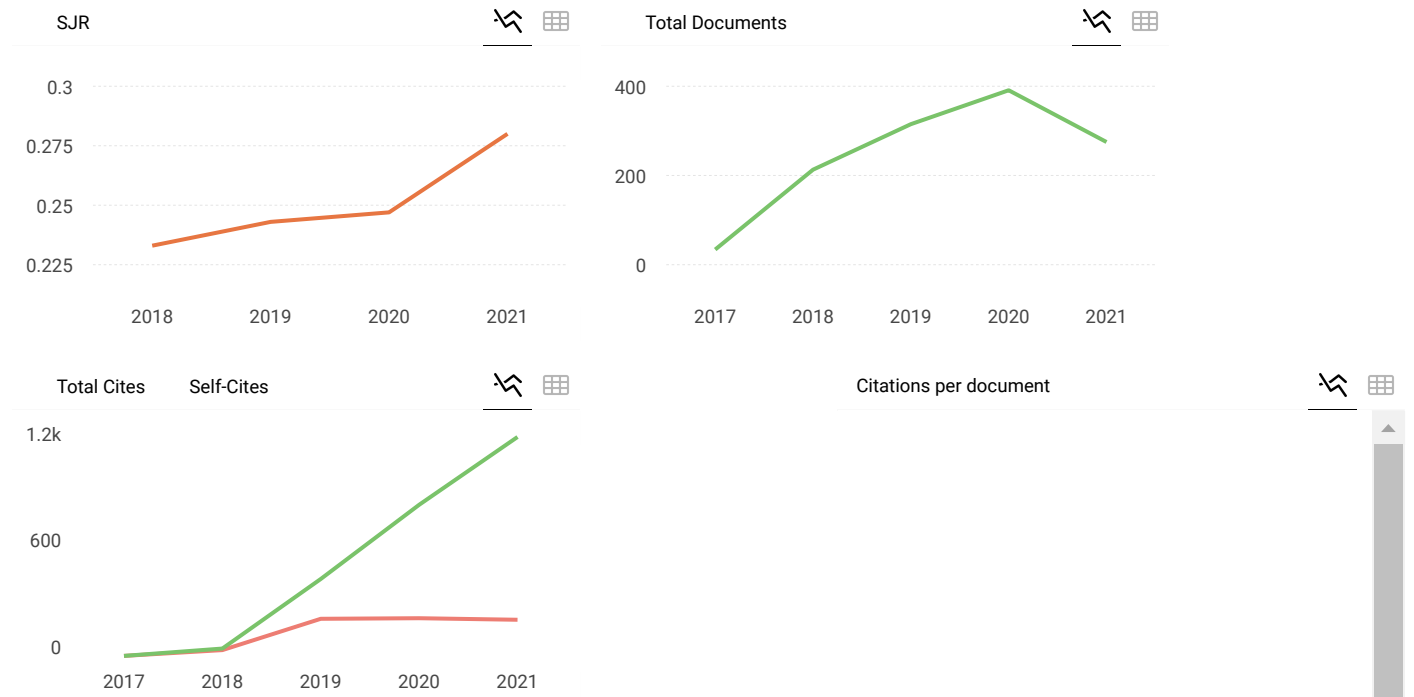


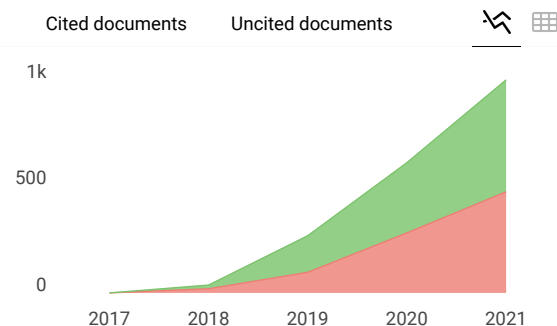
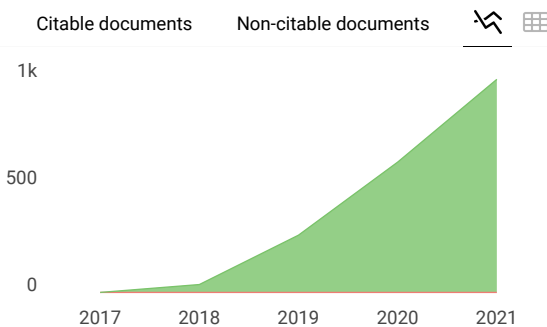
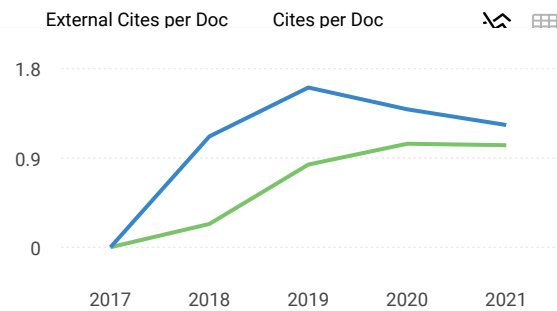
Ad closed by Google

FIND SIMILAR JOURNALS ?

<p>1 CFD Letters MYS 55% similarity</p>	<p>2 Case Studies in Thermal Engineering GBR 54% similarity</p>	<p>3 International Journal of Heat and Technology ITA 50% similarity</p>	<p>4 Thermal Sci Engineering GBR 5 s</p>
--	--	---	---

Ad closed by Google





Journal of Advanced Research in Fluid Mechanics...

Q3 Fluid Flow and Transfer Processes
best quartile

SJR 2021
0.28

powered by scimagojr.com

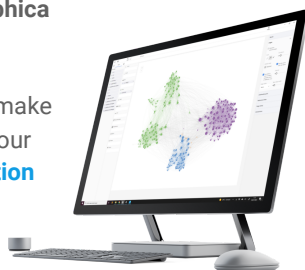
Show this widget in your own website

Just copy the code below and paste within your html code:

```
<a href="https://www.scimaç
```

SCImago Graphica

Explore, visually communicate and make sense of data with our **new data visualization tool**.



Metrics based on Scopus® data as of April 2022

R **Renane Rachid** 2 years ago

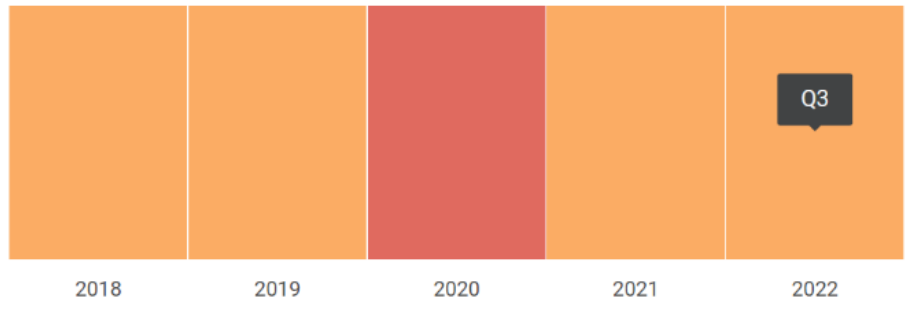
TitlE:AEROHEATING OPTIMISATION OF A HYPERSONIC THERMOCHEMICAL NON-EQUILIBRIUM FLOW AROUND LIFTING BODIES DURING ATMOSPHERIC REENTRY

reply

Quartiles



Fluid Flow and Transfer Processes





Source details

Journal of Advanced Research in Fluid Mechanics and Thermal Sciences

CiteScore 2021

2.2

Scopus coverage years: from 2017 to Present

Publisher: Penerbit Akademia Baru

ISSN: 2289-7879

Subject area: [Chemical Engineering: Fluid Flow and Transfer Processes](#)

SJR 2021

0.280

Source type: Journal

SNIP 2021

0.556[View all documents >](#)[Set document alert](#)[Save to source list](#) [Source Homepage](#)[Locate full-text \(opens in a new window\)](#)[CiteScore](#) [CiteScore rank & trend](#) [Scopus content coverage](#)

Year	Documents published	Actions
2023	85 documents	View citation overview >
2022	362 documents	View citation overview >
2021	280 documents	View citation overview >
2020	391 documents	View citation overview >
2019	315 documents	View citation overview >
2018	213 documents	View citation overview >
2017	34 documents	View citation overview >